Journal Pre-proof

A novel fluorescent probe with dual-sites for simultaneously monitoring metabolisms of cysteine in living cells and zebrafishes

Guoxing Yin, Ting Yu, Yabing Gan, Li Zhou, Meiling Liu, Youyu Zhang, Haitao Li, Peng Yin, Shouzhuo Yao

PII: S1386-1425(20)30581-3

DOI: https://doi.org/10.1016/j.saa.2020.118602

Reference: SAA 118602

To appear in: *Spectrochimica Acta Part A: Molecular and Biomolecular Spectroscopy*

Received date: 13 February 2020

Revised date: 27 May 2020

Accepted date: 8 June 2020

Please cite this article as: G. Yin, T. Yu, Y. Gan, et al., A novel fluorescent probe with dual-sites for simultaneously monitoring metabolisms of cysteine in living cells and zebrafishes, *Spectrochimica Acta Part A: Molecular and Biomolecular Spectroscopy* (2020), https://doi.org/10.1016/j.saa.2020.118602

This is a PDF file of an article that has undergone enhancements after acceptance, such as the addition of a cover page and metadata, and formatting for readability, but it is not yet the definitive version of record. This version will undergo additional copyediting, typesetting and review before it is published in its final form, but we are providing this version to give early visibility of the article. Please note that, during the production process, errors may be discovered which could affect the content, and all legal disclaimers that apply to the journal pertain.

© 2020 Published by Elsevier.

Journal Pre-proof

A Novel Fluorescent Probe with Dual-sites for Simultaneously Monitoring Metabolisms of Cysteine in Living Cells and Zebrafishes

Guoxing Yin,[a] Ting Yu,*[,a] Yabing Gan,[a] Li Zhou,*[,b] Meiling Liu,[a] Youyu Zhang,[a]

Haitao Li,[a] Peng Yin*[a] and Shouzhuo Yao[a]

[a] *Key Laboratory of Chemical Biology and Traditional Chinese Medicine Research (Ministry of Education), College of Chemistry and Chemical Engineering, Hunan Normal University, Changsha 410081, China. E-mail: tingyu@hunnu.edu.cn; yinpeng@hunnu.edu.cn*

[b] *Department of Radiation Oncology, State Key Laboratory of Biotherapy and Cancer Center, West China Hospital, Sichuan University, 610041, China. E-mail: li.zhou@scu.edu.cn*

Abstract

Understanding cellular metabolism holds immense potential for developing new drugs that regulate metabolic pathways. Two gas signal molecules, SO_2 and H_2S, are the main metabolites from cysteine (Cys) via oxidation and desulfurization pathways, respectively. However, a few fluorescent probes for real-time monitor of the metabolic pathways of cysteine have been reported. To understand metabolic alterations of cysteine, we have rationally designed and prepared a dual-signal fluorescent probe **HN**, which could differentiate SO_2 and H_2S through two different fluorescence channels simultaneously, along with similar reaction kinetics and both "off-on" fluorescence responses. Probe **HN** exhibits the potential to monitor the metabolism pathways of cysteine, and the distinguishment of cancer cells from normal cells could be realized. This methodology will promote further understanding of the physiological and pathological roles of cysteine.

Key words: Cysteine, Metabolism pathways, Sulfur dioxide, Hydrogen sulfide, Fluorescent probe

Journal Pre-proof

1. Introduction

Fluorescent probes with multiple reactive sites for multiple analytes have recently attracted lots of interest for occurrences of many physiological and pathological processes are involved in the coincidence of multiple chemical events.[1-8] In order to further understand cellular function and the root causes of diseases, it is therefore crucial to study multiple chemical species simultaneously, and great challenges are existed for simultaneous sensing of structurally similar targets, which also exhibit similar chemical properties.[9,10] Cysteine is a semi-essential proteinogenic amino acid with important functions in redox homeostasis, protein functionality, metabolism, and so on.[11,12] The cellular concentration of cysteine is maintained within a narrow range through its synthesis and degradation. There are two main pathways for the metabolism of cysteine, and two main products were yielded: sulfite (SO_3^{2-}) and hydrogen sulfide (H_2S).[13] As key intermediates, they have major regulatory influences on the homeostasis of cysteine in its related functions.[14,15] The oxidation pathway for cysteine is promoted by cysteine dioxygenase (CDO) and aspartate aminotransferase (AAT), and pyruvate and sulfite would be yielded.[16,17] While, the desulfuration pathway will release sulfane sulfur and hydrogen sulfide (H_2S), which is mainly catalyzed by several enzymes, such as cystathionine β-synthase (CBS) and cystathionine γ-lyase (CSE) (Scheme 1a).[17-20] Abnormal metabolism of cysteine would result in complex diseases including liver damage, Parkinson's and Alzheimer's,[21-25] along with the accumulation of sulfite or H_2S in the body.[26] And besides, endogenous sulfite and H_2S are also biomarkers for differentiating cancer cells and normal cells.[27,28] Therefore, it is of great value to monitor cysteine's important metabolisms sulfite and H_2S simultaneously, and promote deeper understanding of cellular cysteine's functions and the root causes for its related diseases.

Fluorescent probes have becoming powerful tools in determining biologically related species from in vitro to in vivo for they are noninvasive, nondestructive, highly sensitive and relatively simple.[9,29-32] Though several fluorescent probes for discriminating SO_2 and H_2S have been reported,[33-35] to the best of our knowledge, there are few fluorescent probes that could realize the visualization of cysteine's metabolisms in real-time. In 2017, Yin's group reported the first dual-site fluorescent probe for visualizing cysteine and its oxidative metabolism in A-549 cells.[36] Following the pioneering work, Zhang and Ye's groups developed ratiometric and multi-signal mitochondria-targeted fluorescent probes for visualization of cysteine metabolism,[37,38] respectively. However, these probes could not simultaneously monitor of the oxidation and desulfurization metabolism pathways for different concentrations of cysteine from different fluorescence channels. In order to monitor endogenous SO_2 and H_2S from cysteine to illustrate the two metabolic pathways, the design strategies of fluorescent probes would benefit from the following criteria: (1) fluorescent probe could simultaneously

discriminate SO_2 and H_2S from two emission channels with large differences; (2) similar reaction rate constants for sensing SO_2 and H_2S, (3) both "off-on" fluorescence responses towards SO_2 and H_2S.

Generally, *α*,*β*-unsaturated C=C bond was selected as the SO_2 reaction site due to its excellent sensitivity and selectivity,[30,39-42] and the 2,4-dinitrophenyl ether is a typical H_2S sensitive reaction site for H_2S (Scheme 1b).[20,43-47] As a proof of concept, based on the two strategies, we have rationally designed and synthesized a dual-signal fluorescent probe **HN** to visualize the metabolism pathways of cysteine in living cells and zebrafishes. This probe could discriminatively detect SO_2 and H_2S through two fluorescence channels with large emission distance (66 nm). Similar reaction kinetics and dual "off-on" fluorescent signals were also obtained. It was successful to apply this novel probe to monitor the metabolism pathways of cysteine simultaneously in living cells and zebrafishes. This study provides an efficient method to monitor metabolism pathways of cellular cysteine through the sensing of SO_2 and H_2S dynamics and new insights of cellular metabolism and homeostasis were obtained.

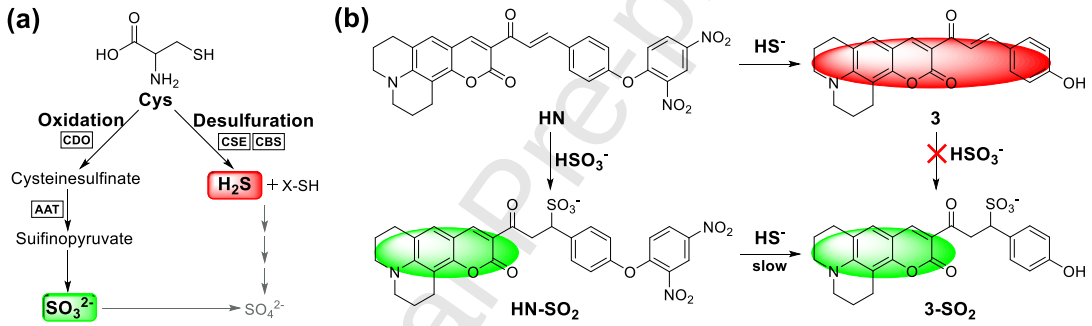

Scheme 1. (a) The two main metabolism pathways of cysteine in mammalian cells. (b) Design of a dual-signal fluorescent probe for monitoring the metabolism pathways of cysteine in real-time.

2. Experimental

2.1. Synthesis of compound 1

Under Argon, fresh distilled DMF (2.8 mL) was added dropwise to $POCl_3$ (2.8 mL) at room temperature and stirred for 30 minutes to yield a red solution. Then a portion of 2,3,6,7-tetrahydro-1*H*,5*H*-pyrido[3,2,1-*ij*]quinolin-8-ol (3.15 g, 16.64 mmol, dissolved in 10 mL DMF) was added dropwise to the above solution and a scarlet suspension was yielded. The mixture was stirred at room temperature for 30 min and 80ºC for 30 min until the reaction was completed, then the reaction mixture was poured into 150 mL of ice water. NaOH solution (20%) was added to adjust the pH to 6 and continue stirred for 2 hours, and a large amount of precipitate was obtained. The crude product was purified by flash column chromatography (PE:EA = 20:1, v/v) to give the product as a brown solid (2.50 g, yield: 69.1%). ^{1}H NMR (500 MHz, $CDCl_3$) δ 11.80 (s, 1H), 9.36 (s, 1H), 6.82 (s, 1H), 3.27 (m, 4H), 2.66 (t, *J* = 6.4, 6.4 Hz, 4H), 1.92 (q, *J* = 6.0, 6.0, 5.9 Hz, 4H). ^{13}C NMR (126 MHz,

Journal Pre-proof

$CDCl_3$) δ 191.66, 159.41, 149.58, 131.25, 113.68, 110.75, 105.35, 50.40, 50.04, 27.32, 21.77, 20.68, 19.75.

2.2. Synthesis of compound 2

To a solution of 8-hydroxy-2,3,6,7-tetrahydro-1*H*,5*H*-pyrido[3,2,1-*ij*]quinoline-9-carbaldehyde (**1**) (1.80 g, 8.28 mmol) and ethyl 3-oxobutanoate (2.16 g, 16.57 mmol) in 20 mL absolute ethanol was added 4-5 drops of piperidine. The reaction mixture was stirred at room temperature for 48 h. After completion of the reaction, the mixture was concentrated to afford the crude product, which was further purified by flash column chromatography to afford the yellow solid (2) (555 mg, 23.4% yield). ^{1}H NMR (500 MHz, $CDCl_3$) δ 8.31 (s, 1H), 6.94 (s, 1H), 3.32 (q, *J* = 5.9, 5.9, 5.8 Hz, 4H), 2.85 (t, *J* = 6.4, 6.4 Hz, 2H), 2.73 (t, *J* = 6.3, 6.3 Hz, 2H), 2.64 (s, 3H), 1.95 (m, 4H). ^{13}C NMR (126 MHz, $CDCl_3$) δ 196.16, 161.42, 153.89, 148.91, 147.94, 127.91, 119.69, 114.91, 108.18, 105.72, 50.47, 50.07, 30.77, 27.55, 21.25, 20.29, 20.17.

2.3. Synthesis of compound 3

To a solution of 10-acetyl-2,3,6,7-tetrahydro-1*H*,5*H*,11*H*-pyrano[2,3-*f*]pyido[3,2,1-*ij*]quinolin-11-one (**2**) (0.50 g, 1.76 mmol) and 4-hydroxybenzaldehyde (539 mg, 4.41 mmol) in 20 mL absolute ethanol was added 2-3 drops of piperidine. The reaction mixture was stirred at 100ºC for 48 h. After completion of the reaction, the cake was filtered and washed with cold ethanol. The solid was dried under vacuum to give the red product (**3**) (0.40 g, 58.5% yield). ^{1}H NMR (500 MHz, DMSO-d_6) δ 10.05 (s, 1H), 8.37 (s, 1H), 7.81 (d, *J* = 15.7 Hz, 1H), 7.56 (m, 3H), 7.19 (s, 1H), 6.83 (d, *J* = 8.1 Hz, 2H), 3.32 (t, *J* = 5.7, 5.7 Hz, 4H), 2.70 (m, 4H), 1.86 (m, 4H). ^{13}C NMR (126 MHz, DMSO-d_6) δ 185.63, 160.58, 160.34, 153.39, 148.98, 148.26, 142.57, 130.83, 128.23, 126.52, 122.23, 119.86, 116.42, 114.77, 108.13, 105.05, 50.13, 49.61, 27.23, 20.99, 20.02.

2.4. Synthesis of probe HN

To a solution of (*E*)-10-(3-(4-hydroxyphenyl)acryloyl)-2,3,6,7-tetrahydro-1*H*,5*H*,11*H*-pyrano[2,3-*f*]pyrido[3,2,1-*ij*]quinolin-11-one (**3**) (0.20 g, 0.516 mmol) in 20 mL anhydrous acetonitrile was added 1-fluoro-2,4-dinitrobenzene (115mg, 0.619 mmol). The reaction mixture was stirred at room temperature for 2 min, then a few drops of triethylamine was added. After completion of the reaction, the cake was filtered and washed with cold acetonitrile. The solid was dried under vacuum and further purified by flash column chromatography to give the red product (probe **HN**) (175 mg, 61.2% yield). ^{1}H NMR (500 MHz, $CDCl_3$) δ 8.85 (d, *J* = 2.8 Hz, 1H), 8.46 (s, 1H), 8.34 (dd, *J* = 9.0, 2.8 Hz, 1H), 8.18 (d, *J* = 15.7 Hz, 1H), 7.77 (m, 3H), 7.15 (d, *J* = 8.2 Hz, 2H), 7.10 (d, *J* = 9.3 Hz, 1H), 7.01 (s, 1H),

3.36 (q, *J* = 5.2, 5.2, 5.2 Hz, 4H), 2.89 (t, *J* = 6.3, 6.3 Hz, 2H), 2.77 (t, *J* = 6.2, 6.2 Hz, 2H), 1.99 (m, 4H). ^{13}C NMR (126 MHz, $CDCl_3$) δ 186.56, 161.56, 155.83, 154.87, 153.96, 149.17, 149.01, 141.88, 140.70, 139.88, 134.30, 131.00, 129.04, 128.01, 126.49, 122.30, 120.85, 119.92, 119.11, 115.11, 108.77, 105.83, 50.58, 50.18, 27.59, 21.28, 20.32, 20.20. IR (KBr pellet, cm^{-1}): 3029, 2925, 2854, 1718, 1610, 1513, 1438, 1381, 1311 1267, 1192, 1132, 1052, 816, 696. HRMS: m/z $[M + H]^+$ calculated for $C_{30}H_{24}N_3O_8$: 554.1558; measured: 554.1568.

2.5. Cell culture.

HepG2 and L-O2 cells were obtained from China Center for Type Culture Collection (Wuhan, China). The cells were incubated in Dulbecco's modified Eagle's medium (DMEM) with 10% (v/v) heat-inactivated fetal bovine serum (FBS) (Gibco BRL, Grand Island, NY, USA), streptomycin-penicillin (100 U/mL, 100 μg/mL) in a humidified incubator of 5% CO_2 and 95% air at 37°C.

2.6. Imaging of endogenous and exogenous SO_2 and H_2S (metabolisms of cysteine) in living cells.

For the detection of SO_2 and H_2S in cells, HepG2 and L-O2 and were incubated with probe (10 μM) for 60 min, then imaged after washing by phosphate-buffered saline (PBS) for three times. To detect exogenous SO_2 and H_2S, HepG2 and L-O2 cells were pretreated with NEM (0.25 mM) for 30 min, subsequently incubated with Cys (50, 100, 200, 400, 800, 1000 μM, 60 min) and probe **HN** (10 μM, 60 min), then washed with phosphate-buffered saline (PBS) for three times. Cells were imaged by a fluorescence confocal microscope (Leica SP8, Germany). (λ_{ex} = 458 nm, λ_{em} = 480 - 550 nm for the green channel; and λ_{ex} = 514 nm, λ_{em} = 560 - 650 nm for the red channel).

2.7. Imaging of SO_2 and H_2S (metabolisms of cysteine) in living zebrafish.

For the detection of metabolisms of cysteine (SO_2 and H_2S) in vivo, 3-day-old zebrafishes were prepared. To detect endogenous SO_2 and H_2S, the zebrafishes incubated with probe (10 μM) for 60 min, then imaged. Fluorescent Imaging of Cys metabolisms in zebrafishes, zebrafishes were fed with 250 μM NEM in E3 embryo media (15 mM NaCl, 0.5 mM KCl, 1 mM $MgSO_4$, 1 mM $CaCl_2$, 0.15 mM KH_2PO_4, 0.05 mM Na_2HPO_4, 0.7 mM $NaHCO_3$, 10^{-5}% methylene blue; pH 7.5) at 28 °C for 30 min, then incubated with Cys (600 μM, 60 min), and finally incubated with probe (10 μM) for 60 min. All the fishes were terminally anaesthetized using MS222, and images were carried out on a confocal microscope. (Leica SP8, Germany). (λ_{ex} = 458 nm, λ_{em} = 480 - 550 nm for the green channel; and λ_{ex} = 514 nm, λ_{em} = 560 - 650 nm for the red channel).

Journal Pre-proof

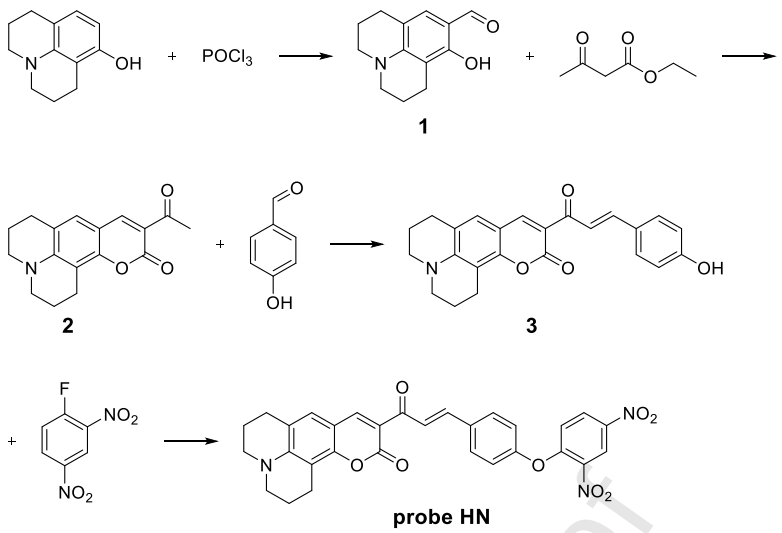

Scheme 2. Synthesis of the probe **HN**.

3. Results and Discussions

3.1 Spectral responses of probe HN toward SO_2 and H_2S

Firstly, the UV-vis and fluorescent responses of probe **HN** toward reactive sulfur species (thiols, $NaHSO_3$ and NaHS) were measured carefully in DMSO/PBS (pH 7.4, 10 mM, v/v, 5/5) at 30 °C for 30 min. As expected, upon addition of $NaHSO_3$, the initial absorption peak at 499 nm was changed to 470 nm with a 29 nm blue shift, which should be attributed to the addition of $NaHSO_3$ to the C=C double bond (Fig. S1a, Fig. S2). Correspondingly, a significant fluorescence turn-on at 515 nm was observed at 460 nm excitation (Fig. 1a, Φ: 0.10 with fluorescein as reference), while other competitive analytes induced little fluorescence. On the other hand, for NaHS, a slightly redshifted absorption band and a clear fluorescence enhancement at 581 nm were observed due to the thiolysis of 2,4-dinitrophenyl ethers induced by NaHS (Fig. 1b, Fig. S1, S3, Φ: 0.06 with fluorescein as reference). Thus, the probe **HN** could differentiate SO_2 and H_2S from two fluorescence channels with large distance (66 nm) without interferences from biothiols, for the specific reaction sites for SO_2 and H_2S were properly established in the probe **HN**. More importantly, the sensing of $NaHSO_3$ and NaHS with probe **HN** was followed by pseudo-first-order kinetics: k_{obs} = 0.07 min^{-1} and a half-life of 10.0 min for $NaHSO_3$; k_{obs} = 0.09 min^{-1} and a half-life of 7.4 min for NaHS based on a global fitting for the fluorescence growth at 515 and 581 nm, respectively (Fig. 1c, 1d).[48,49] The results from pH titration have showed that detection of $NaHSO_3$ and NaHS could be realized over a broad pH range (Fig. S4). All of the results have indicated that probe **HN** could simultaneously monitor the two metabolites of cysteine: SO_2 and H_2S, from two different emission channels.

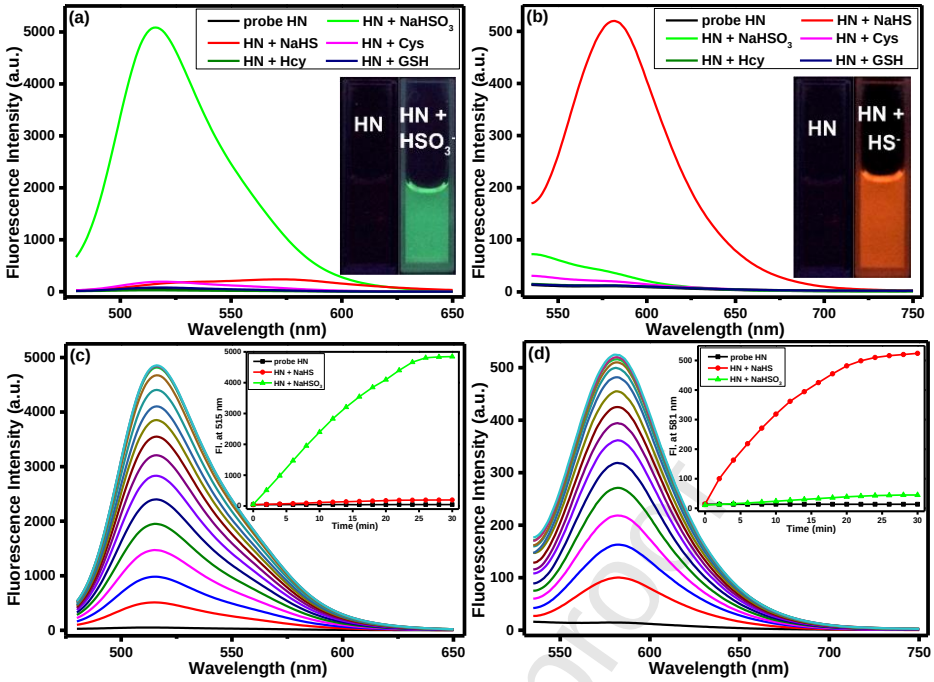

Fig. 1. (a-b) Fluorescence spectra of probe **HN** (10 μM) upon addition of 10 equiv. of Cys, Hcy, GSH, NaHS and $NaHSO_3$ (100 μM) for 30 min. Inset: The inset photos show color changes of probe **HN** in the absence and presence of (a) $NaHSO_3$, (b) NaHS under UV lamp at 365 nm. (c-d) Time-dependent fluorescence spectra of probe **HN** (10 μM) in the presence of 10 equiv. of (c) $NaHSO_3$, (d) NaHS. Inset: the corresponding time-dependent fluorescence intensity changes at (c) 515 nm, (d) 581 nm. Conditions: DMSO-PBS (pH 7.4, 10 mM, v/v, 5/5), Temperature: 30 °C. (a, c) λ_{ex} = 460 nm, (b, d) λ_{ex} = 500 nm. Slit (nm): 2.5/5.

3.2. Selectivity and sensitivity of probe HN for SO_2 and H_2S

Next, we assessed the selectivity of probe **HN** over other biologically related or environmentally important species, such as Cys (0.2 mM), GSH (2.5 mM), and Hcy (0.1 mM) in DMSO-PBS (pH 7.4, 10 mM, v/v, 5/5) at 30°C for 60 min. Encouragingly, except $NaHSO_3$ and NaHS, addition of other analytes resulted in no remarkable fluorescence enhancement at 515 and 581 nm excited at 460 and 500 nm, respectively (Fig. S5, S6). Therefore, probe **HN** could detect $NaHSO_3$ and NaHS with high selectivity even in the existence of high concentrations of thiols. The fluorescence enhancement at 515 nm and 581 nm showed good linear relationship (R^2 > 0.99) to the concentration of HSO_3^- and HS^- (Fig. S7, S8), and the detection limit were calculated to be as low as 20 and 120 nM for HSO_3^- and HS^- based on IUPAC definition (LOD = 3σ/S), respectively. These results clearly demonstrated this novel dual-function probes could simultaneously discriminate two analytes from two emission channels with large distance (> 50 nm), along with excellent chemical stability under physiological conditions.

3.3. Mechanism of probe HN with SO_2 and H_2S.

As shown in scheme 1b, to verify whether the spectroscopic differences in the responses of probe **HN** toward $NaHSO_3$ and NaHS were caused by the different sensing mechanisms as designed. The compound **3** and **HN-SO_2** were easily isolated and characterized well by NMR analyses (Figs. S29-S32). The product **3-SO_2** (Φ: 0.58 with fluorescein as reference) was also successfully obtained from the reaction between compound **3** with $NaHSO_3$ (Figs. S33-S35). The absorption and fluorescence spectra of isolated products were well studied (Fig. S1), which were consistent with the proposed mechanism. In addition, theoretical calculations showed that the product **3** from the reaction between **HN** and H_2S exhibited a bigger energy gap between the HOMO (highest occupied molecular orbital) and LUMO (lowest unoccupied molecular orbital) (3.40 eV) than that of **HN** (2.41 eV) (Fig. S16), which indicated that compound **3** will be more difficult to react with SO_2 to afford the compound **3-SO_2**, which further supports the sensing mechanism of probe **HN** with both "off-on" fluorescence response toward SO_2 and H_2S. Thus, probe **HN** could simultaneously react with SO_2 and H_2S to afford different spectroscopic properties of compound **3** and **HN-SO_2**, respectively.

The responses of compound **3** toward representative relevant species were also performed. Almost no significant changes were observed in the time-dependent absorption spectra and fluorescence intensities (515 nm) after it was treated with 20 equiv. of reactive sulfur species (Cys, GSH and Hcy *et al*.) within a short time (Fig. S9). Meanwhile, it was clear that using different excitations the mixture of $NaHSO_3$, NaHS, Cys, Hcy and GSH could elicit dramatic fluorescence enhancement within their specific channels (Fig. S10-S12). Furthermore, in presence of H_2S, **HN-SO_2** was transformed to product **3-SO_2** very slowly (Fig. S13, S14). To confirm the bioavailability of probe **HN**, we have also examined their photostability under the same conditions. Solutions of probe **HN**, **HN-SO_2** and compound **3** were continuously irradiated via a Xe-lamp at 460 and 500 nm wavelengths, respectively. It was observed that all compounds were stable after continuous irradiation for 2h (> 95% of the initial values for compound **HN-SO_2** and compound **3**) (Fig. S15). Therefore, these experiments well demonstrated that probe **HN** could be applied to simultaneously sense SO_2 and H_2S from two fluorescence channels with continuous fluorescence signal retention, and it would be an excellent tool for monitoring the metabolism pathways of cysteine in vivo in real-time.

3.4. Fluorescent Imaging of SO_2 and H_2S in Living Cells.

Encouraging by the aforementioned results, the practicality of probe **HN** for imaging metabolites of cysteine was evaluated in biological environment. Firstly, probe **HN** was found to be low toxic for living cells, which was evaluated by the standard CCK-8 assay (Fig. S17). After pretreated with N-ethylmaleimide (NEM, scavenger of SH compounds), Cells exhibited no fluorescence in both green and red channels after incubation with probe **HN** for 2 h(Fig. S18). However, when treatment with

exogenous $NaHSO_3$ (Fig. 2A-B) and NaHS (Fig. 2C-D) in the NEM-pretreated HepG2 cells significant fluorescence in the green and red channel were observed after incubated with **HN** for 10 min, respectively. Application of probe **HN** for simultaneous visualization of endogenous SO_2 and H_2S in cancer cells (HepG2) and normal cells (L-O2) were then conducted. The L-O2 cells were exhibited bright red and weak green fluorescence after stained with **HN** for 60 min simultaneously (Fig. 3A1-B1), while HepG2 cells were shown brighter green fluorescence (Fig. S19, A1-B1), which indicated that different levels of sulfite and H_2S are existed in the normal cells and cancer cells. Therefore, probe **HN** could be applied to image the endogenous and exogenous SO_2 and H_2S through two different fluorescence channels with high selectivity and high sensitivity. And the discrimination of normal and cancer cells could be realized through the monitor of the metabolites of cysteine.

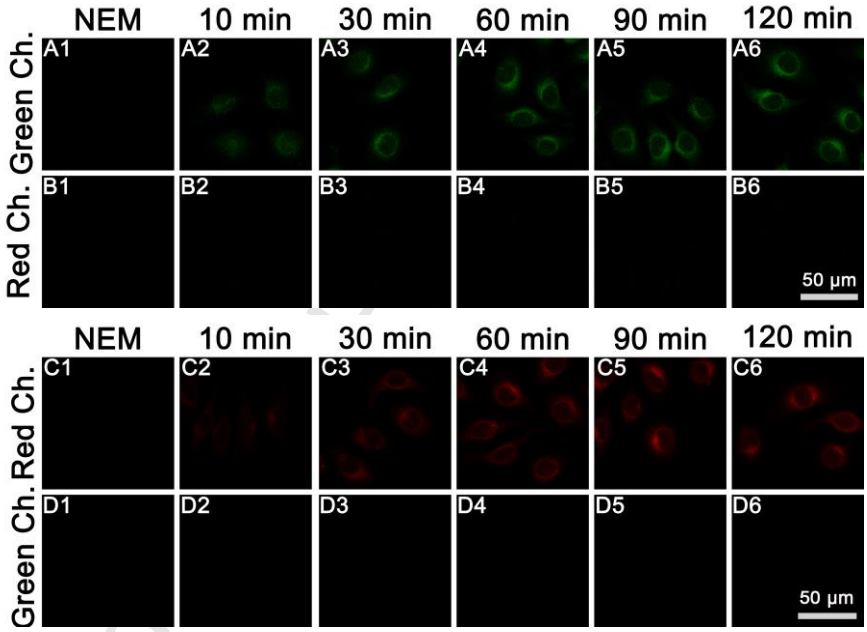

Fig. 2. Confocal fluorescence images of SO_2 and H_2S in HepG2 cells. A-D). Cells were pretreated with NEM (0.25 mM, 30 min), then treated with probe **HN** (10 μM, 30 min) and $NaHSO_3$ (A-B), NaHS (C-D) (250 μM) for 10, 30, 60, and 90 min, respectively, then imaged. (λ_{ex} = 458 nm, λ_{em} = 480 - 550 nm for the green channel; and λ_{ex} = 514 nm, λ_{em} = 560 - 650 nm for the red channel). Scale bar: 50 μm.

3.5. Fluorescence imaging of metabolism pathways of cysteine in living cells and zebrafish

Subsequently, based on its efficient sensing capability for SO_2 and H_2S in living cells, probe **HN** was applied to monitor the metabolism pathways of cysteine. L-O2 cells were first treated with NEM (250 μM) for 60 min, and then treated with different concentration of Cys (50, 100, 200, 400, 800 and 1000 μM) for another 60 min. As showed in Fig. 3, L-O2 cells were exhibited brighter red fluorescence after incubated low concentration of Cys (50 μM, Fig. 3A2-B2). However, fluorescence in green channel

was significantly increased along with the increasement of the concentration of Cys. Fluorescence imaging of metabolites of cysteine were also performed in HepG2 cells (Fig. S19), and similar results were obtained. Moreover, sensing of metabolism pathways of cysteine in zebrafish with probe **HN** was conducted. After pretreated with NEM, zebrafish was illustrated no fluorescence in both the green and red channels after incubated with probe **HN** (Fig. 4, A1−C1). However, endogenous SO_2 and H_2S in zebrafish could be sensed simultaneously from two different fluorescence channels (Fig. 4, A2, B2). After further treated with Cys, significant fluorescence enhancement in the green channels could be observed, which reflected more endogenous bisulfite/sulfite (Fig. 4, A2−A7, Fig. S20) were released. The results demonstrated that probe **HN** could monitor H_2S and SO_2 in real-time, which are produced from Cys metabolism in living cells and zebrafish. And the differences in fluorescence intensities indicated that desulfuration pathway would be dominate when cysteine is deficient, whereas oxidative metabolism would be the main pathway when cysteine is in excess (Fig. 3B; Fig. S20).[13-15]

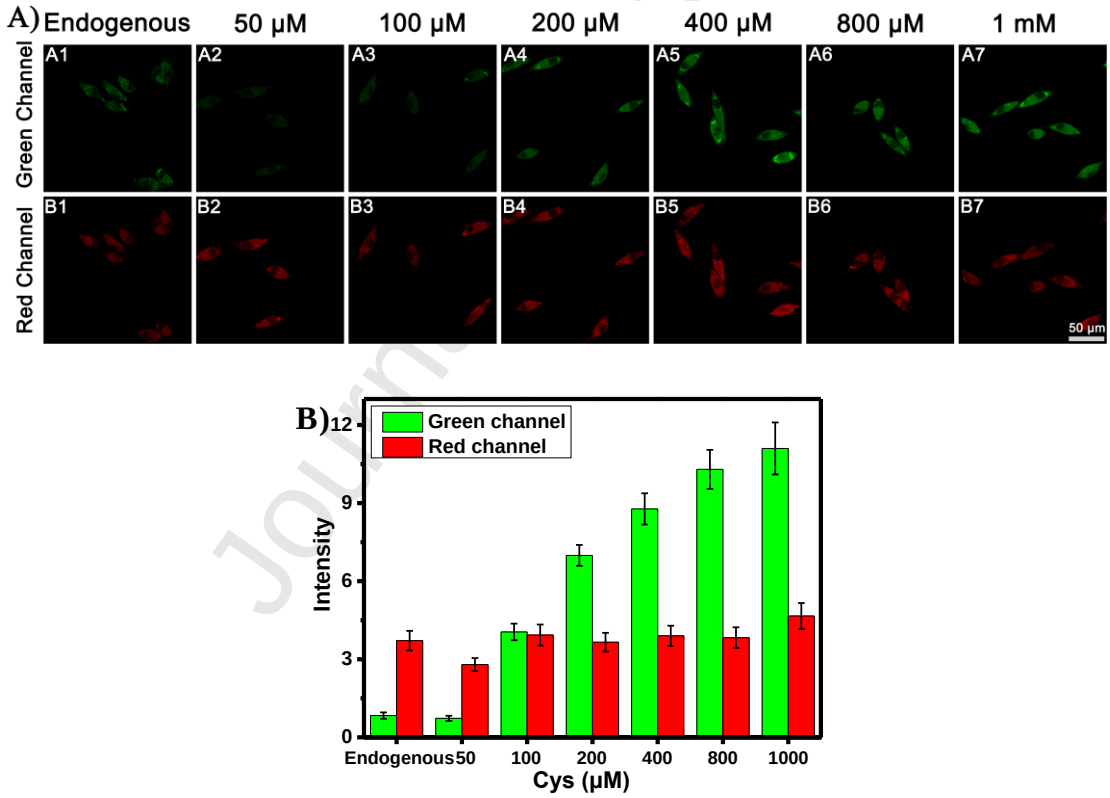

Fig. 3. Confocal fluorescence images of metabolisms of cysteine in L-O2 cells. Cells were incubated with probe **HN** (10 μM) for 60 min, then imaged (A1-B1). Cells were pretreated with NEM (250 μM, 30 min), then incubated with 50, 100, 200, 400, 800, 1000 μM Cys for 60 min, respectively, and finally incubated with probe (10 μM) for 60 min (A2-B7). (B) The intensity of green and red channel in Fig. A1-B7. (λ_{ex} = 458 nm, λ_{em} = 480 - 550 nm for the green channel; and λ_{ex} = 514 nm, λ_{em} = 560 - 650 nm for the red channel). Scale bar: 50 μm. The fluorescence intensity was calculated by Leica LAS X

program. Scale bar: 50 μm.

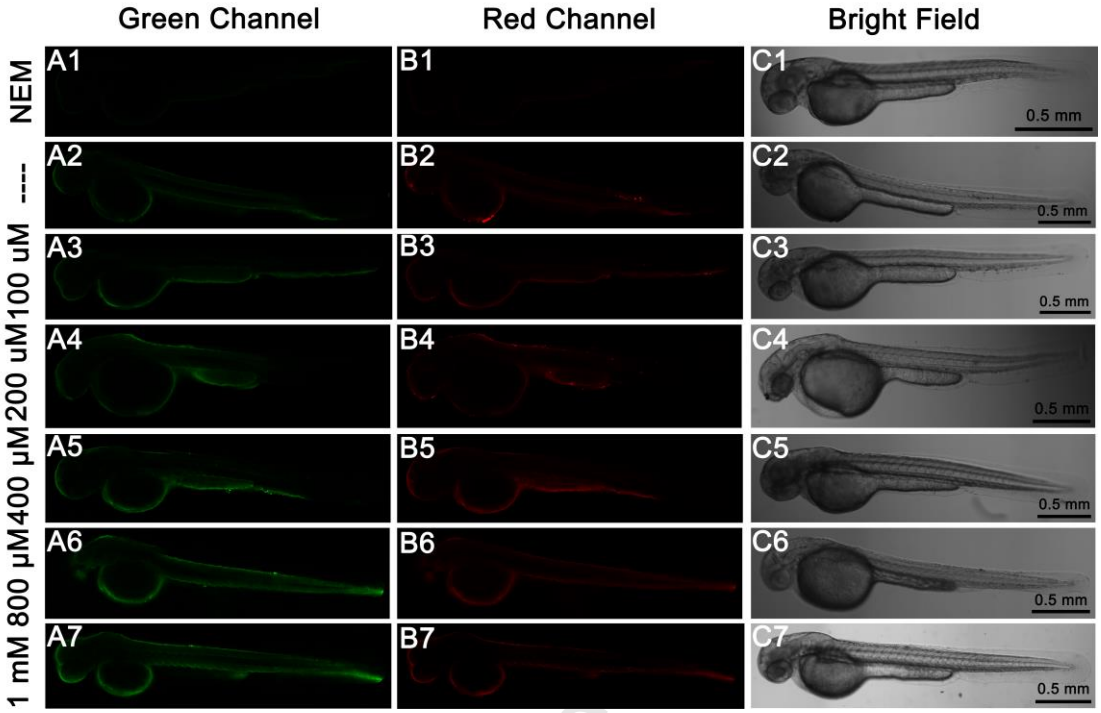

Fig. 4. Confocal fluorescence images of metabolisms of cysteine in zebrafishes. Zebrafish was pretreated with NEM (250 μM, 30 min), then incubated with probe **HN** (10 μM) for 60 min, and finally imaged (A1-C1). Zebrafish was incubated with probe **HN** (10 μM) for 60 min, then imaged (A2-C2). Zebrafish was pretreated with NEM (250 μM, 30 min), then incubated with Cys (100, 200, 400, 800 and 1000 μM, respectively, 60 min), and finally incubated with probe (10 μM) for 60 min, then imaged (A3-A7). (λ_{ex} = 458 nm, λ_{em} = 480 - 550 nm for the green channel; and λ_{ex} = 514 nm, λ_{em} = 560 - 650 nm for the red channel). Scale bar: 0.5 mm.

4. Conclusion

In conclusion, we have rationally developed a dual-signal fluorescent probe for monitoring the metabolism pathways of cysteine in real-time. For the simultaneous detection of $NaHSO_3$ and NaHS, the probe **HN** was featured with large emission differences (66 nm), similar reaction rate constants and sustained fluorescence signals. This probe was successfully applied to the simultaneous imaging SO_2 and H_2S from different emission channels. Importantly, probe **HN** could be used to monitor the metabolism pathways of cysteine. Pathways of desulfurization or oxidation are mainly depended on the concentrations of cysteine. This methodology will provide better understanding for the physiological and pathological roles of cysteine, and further promote the diagnosis and treatment of diseases, which are related to cysteine and its metabolites.

Conflicts of interest

The authors declare no competing financial interest.

Acknowledgements

This work was supported by the funding from the National Natural Science Foundation of China (Grant No. 21877035, 21977028 and 11905150); Research Foundation of Education Bureau of Hunan Province (No. 18B004) and Sichuan Science and Technology Program (2018HH0099).

References

[1] Y. Yue, F. Huo, F. Cheng, X. Zhu, T. Mafireyi, R.M. Strongin, C. Yin, Functional synthetic probes for selective targeting and multi-analyte detection and imaging, Chem. Soc. Rev. 48 (2019) 4155-4177.

[2] G.-x. Yin, T.-t. Niu, Y.-b. Gan, T. Yu, P. Yin, H.-m. Chen, Y.-y. Zhang, H.-t. Li, S.-z. Yao, A Multi-signal Fluorescent Probe with Multiple Binding Sites for Simultaneous Sensing of Cysteine, Homocysteine, and Glutathione, Angew. Chem. Int. Ed. 57 (2018) 4991-4994.

[3] G. Yin, T. Niu, T. Yu, Y. Gan, X. Sun, P. Yin, H. Chen, Y. Zhang, H. Li, S. Yao, Simultaneous Visualization of Endogenous Homocysteine, Cysteine, Glutathione, and their Transformation through Different Fluorescence Channels, Angew. Chem. Int. Ed. 58 (2019) 4557-4561.

[4] M. Kunitski, N. Eicke, P. Huber, J. Köhler, S. Zeller, J. Voigtsberger, N. Schlott, K. Henrichs, H. Sann, F. Trinter, L.P.H. Schmidt, A. Kalinin, M.S. Schöffler, T. Jahnke, M. Lein, R. Dörner, Double-slit photoelectron interference in strong-field ionization of the neon dimer, Nat. Commun. 10 (2019) 1.

[5] W. Chen, T. Matsunaga, D.L. Neill, C.-t. Yang, T. Akaike, M. Xian, Rational Design of a Dual-Reactivity-Based Fluorescent Probe for Visualizing Intracellular HSNO, Angew. Chem. Int. Ed. 58 (2019) 16067-16070.

[6] H. Li, W. Shi, X. Li, Y. Hu, Y. Fang, H. Ma, Ferroptosis Accompanied by •OH Generation and Cytoplasmic Viscosity Increase Revealed via Dual-Functional Fluorescence Probe, J. Am. Chem. Soc. 141 (2019) 18301-18307.

[7] Z. Li, S. Huang, Y. He, Q. Duan, G. Zheng, Y. Jiang, L. Cai, Y. Jia, H. Zhang, D. Ho, AND logic gate based fluorescence probe for simultaneous detection of peroxynitrite and hypochlorous acid, Spectrochim. Acta. A Mol. Biomol. Spectrosc. 230 (2020) 118073.

[8] Y. Li, L. Liu, Y. Tang, Y. Wang, J. Han, L. Ni, A new colorimetric and ratiometric probe for highly selective recognition and bioimaging of ClO^- and Al^{3+}, Spectrochim. Acta. A Mol. Biomol. Spectrosc. 232 (2020) 118154.

[9] J.L. Kolanowski, F. Liu, E.J. New, Fluorescent probes for the simultaneous detection of multiple analytes in biology, Chem. Soc. Rev. 47 (2018) 195-208.

[10] A. Romieu, "AND" luminescent "reactive" molecular logic gates: a gateway to multi-analyte bioimaging and biosensing, Org. Biomol. Chem. 13 (2015) 1294-1306.

Journal Pre-proof

[11] B.D. Paul, J.I. Sbodio, S.H. Snyder, Cysteine Metabolism in Neuronal Redox Homeostasis, Trends Pharmacol. Sci. 39 (2018) 513-524.

[12] R.C. Geck, A. Toker, A. Nonessential amino acid metabolism in breast cancer, Adv. Biol. Regul. 62 (2016) 11-17.

[13] M.H. Stipanuk, J.E. Dominy, Jr., J.-I. Lee, R.M. Coloso, Mammalian Cysteine Metabolism: New Insights into Regulation of Cysteine Metabolism, J. Nutr. 136 (2006) 1652S-1659S.

[14] J.B. Kohl, A.-T. Mellis, G. Schwarz, Homeostatic impact of sulfite and hydrogen sulfide on cysteine catabolism, Br. J. Pharmacol.176 (2019) 554-570.

[15] M.H. Stipanuk, I. Ueki, Dealing with methionine/homocysteine sulfur: cysteine metabolism to taurine and inorganic sulfur, J. Inherit. Metab. Dis. 34 (2011) 17-32.

[16] T. Ubuka, J. Ohta, W.-B. Yao, T. Abe, T. Teraoka, Y. Kurozumi, l-Cysteine metabolism via 3-mercaptopyruvate pathway and sulfate formation in rat liver mitochondria, Amino Acids 2 (1992) 143-155.

[17] X. Li, F.W. Bazer, H. Gao, W. Jobgen, G.A. Johnson, P. Li, J.R. McKnight, M.C. Satterfield, T.E. Spencer, G. Wu, Amino acids and gaseous signaling, Amino Acids 37 (2009) 65-78.

[18] L. Yi, L. Wei, R. Wang, C. Zhang, J. Zhang, T. Tan, Z. Xi, A Dual-Response Fluorescent Probe Reveals the H_2O_2-Induced H_2S Biogenesis through a Cystathionine β-Synthase Pathway, Chem. Eur. J. 21 (2015) 15167-15172.

[19] M.R. Filipovic, J. Zivanovic, B. Alvarez, R. Banerjee, Chemical Biology of H_2S Signaling through Persulfidation, Chem. Rev. 118 (2018) 1253-1337.

[20] V.S. Lin, W. Chen, M. Xian, C.J. Chang, Chemical probes for molecular imaging and detection of hydrogen sulfide and reactive sulfur species in biological systems, Chem. Soc. Rev. 44 (2015) 4596-4618.

[21] X. Chen, Y. Zhou, X. Peng, J. Yoon, Fluorescent and colorimetric probes for detection of thiols, Chem. Soc. Rev. 39 (2010) 2120-2135.

[22] X. Jiao, Y. Li, J. Niu, X. Xie, X. Wang, B. Tang, Small-Molecule Fluorescent Probes for Imaging and Detection of Reactive Oxygen, Nitrogen, and Sulfur Species in Biological Systems, Anal. Chem. 90 (2018) 533-555.

[23] C. Hine, E. Harputlugil, Y. Zhang, C. Ruckenstuhl, Byung C. Lee, L. Brace, A. Longchamp, Jose H. Treviño-Villarreal, P. Mejia, C.K. Ozaki, R. Wang, Vadim N. Gladyshev, F. Madeo, William B. Mair, James R. Mitchell, Endogenous Hydrogen Sulfide Production Is Essential for Dietary Restriction Benefits, Cell 160 (2015) 132-144.

Journal Pre-proof

[24] L. He, X. Yang, K. Xu, X. Kong, W. Lin, A multi-signal fluorescent probe for simultaneously distinguishing and sequentially sensing cysteine/homocysteine, glutathione, and hydrogen sulfide in living cells, Chem. Sci. 8 (2017) 6257-6265.

[25] H. Chen, Y. Tang, M. Ren, W. Lin, Single near-infrared fluorescent probe with high- and low-sensitivity sites for sensing different concentration ranges of biological thiols with distinct modes of fluorescence signals, Chem. Sci. 7 (2016) 1896-1903.

[26] M.-B. Marcos, Cysteine Network (CYSTEINET) Dysregulation in Parkinson's Disease: Role of *N*-acetylcysteine, Curr. Drug Metab. 17 (2016) 368-385.

[27] D.-P. Li, Z.-Y. Wang, X.-J. Cao, J. Cui, X. Wang, H.-Z. Cui, J.-Y. Miao, B.-X. Zhao, A mitochondria-targeted fluorescent probe for ratiometric detection of endogenous sulfur dioxide derivatives in cancer cells, Chem. Commun. 52 (2016) 2760-2763.

[28] D.-P. Li, Z.-Y. Wang, H. Su, J.-Y. Miao, B.-X. Zhao, Fluorescence detection of endogenous bisulfite in liver cancer cells using an effective ESIPT enhanced FRET platform, Chem. Commun. 53 (2017) 577-580.

[29] K.Y. Zhang, Q. Yu, H. Wei, S. Liu, Q. Zhao, W. Huang, Long-Lived Emissive Probes for Time-Resolved Photoluminescence Bioimaging and Biosensing, Chem. Rev. 118 (2018) 1770-1839.

[30] K. Li, L.-L. Li, Q. Zhou, K.-K. Yu, J.S. Kim, X.-Q. Yu, Reaction-based fluorescent probes for SO_2 derivatives and their biological applications, Coordin. Chem. Rev. 388 (2019) 310-333.

[31] P. Gao, W. Pan, N. Li, B. Tang, Fluorescent probes for organelle-targeted bioactive species imaging, Chem. Sci. 10 (2019) 6035-6071.

[32] D. Cao, Z. Liu, P. Verwilst, S. Koo, P. Jangjili, J.S. Kim, W. Lin, Coumarin-Based Small-Molecule Fluorescent Chemosensors, Chem. Rev. 119 (2019) 10403-10519.

[33] H. Tian, J. Qian, Q. Sun, C. Jiang, R. Zhang, W. Zhang, A coumarin-based fluorescent probe for differential identification of sulfide and sulfite in CTAB micelle solution, Analyst 139 (2014) 3373-3377.

[34] X. Pei, H. Tian, W. Zhang, A.M. Brouwer, J. Qian, Colorimetric and fluorescent determination of sulfide and sulfite with kinetic discrimination, Analyst 139 (2014) 5290-5296.

[35] S. Chen, C. Ma, M.-S. Yuan, W. Wang, D.-E. Wang, S.-W. Chen, J. Wang, A dual functional probe: sensitive fluorescence response to H_2S and colorimetric detection for SO_3^{2-}. RSC Adv. 6 (2016) 85529-85537.

[36] Y. Yue, F. Huo, P. Ning, Y. Zhang, J. Chao, X. Meng, C. Yin, Dual-Site Fluorescent Probe for Visualizing the Metabolism of Cys in Living Cells, J. Am. Chem. Soc. 139 (2017) 3181-3185.

Journal Pre-proof

[37] B. Xu, H. Zhou, Q. Mei, W. Tang, Y. Sun, M. Gao, C. Zhang, S. Deng, Y. Zhang, Real-Time Visualization of Cysteine Metabolism in Living Cells with Ratiometric Fluorescence Probes, Anal. Chem. 90 (2018) 2686-2691.

[38] X. Yang, W. Liu, J. Tang, P. Li, H. Weng, Y. Ye, M. Xian, B. Tang, Y. Zhao, A multi-signal mitochondria-targeted fluorescent probe for real-time visualization of cysteine metabolism in living cells and animals, Chem. Commun. 54 (2018) 11387-11390.

[39] L.E. Santos-Figueroa, C. Giménez, A. Agostini, E. Aznar, M.D. Marcos, F. Sancenón, R. Martínez-Máñez, P. Amorós, Selective and Sensitive Chromofluorogenic Detection of the Sulfite Anion in Water Using Hydrophobic Hybrid Organic–Inorganic Silica Nanoparticles, Angew. Chem. Int. Ed. 52 (2013) 13712-13716.

[40] Y.-Q. Sun, J. Liu, J. Zhang, T. Yang, W. Guo, Fluorescent probe for biological gas SO_2 derivatives bisulfite and sulfite, Chem. Commun. 49 (2013) 2637-2639.

[41] M. Moccia, F. Fini, M. Scagnetti, M.F.A. Adamo, Catalytic Enantioselective Addition of Sodium Bisulfite to Chalcones, Angew. Chem. Int. Ed. 50 (2011) 6893-6895.

[42] G. Yin, Y. Gan, T. Yu, T. Niu, P. Yin, H. Chen, Y. Zhang, H. Li, S. Yao, A dual-emission and mitochondria-targeted fluorescent probe for rapid detection of SO_2 derivatives and its imaging in living cells, Talanta 191 (2019) 428-434.

[43] C. Zhang, L. Wei, C. Wei, J. Zhang, R. Wang, Z. Xi, L. Yi, A FRET–ICT dual-quenching fluorescent probe with large off–on response for H_2S: synthesis, spectra and bioimaging, Chem. Commun. 51 (2015) 7505-7508.

[44] J. Wang, W. Lin, W. Li, Three-channel fluorescent sensing via organic white light-emitting dyes for detection of hydrogen sulfide in living cells, Biomaterials 34 (2013) 7429-7436.

[45] X. Cao, W. Lin, K. Zheng, L. He, A near-infrared fluorescent turn-on probe for fluorescence imaging of hydrogen sulfide in living cells based on thiolysis of dinitrophenyl ether, Chem. Commun. 48 (2012) 10529-10531.

[46] T. Liu, Z. Xu, D.R. Spring, J. Cui, A Lysosome-Targetable Fluorescent Probe for Imaging Hydrogen Sulfide in Living Cells, Org. Lett. 15 (2013) 2310-2313.

[47] F. Yu, X. Han, L. Chen, Fluorescent probes for hydrogen sulfide detection and bioimaging, Chem. Commun. 50 (2014) 12234-12249.

[48] X. Jiang, Y. Yu, J. Chen, M. Zhao, H. Chen, X. Song, A.J. Matzuk, S.L. Carroll, X. Tan, A. Sizovs, N. Cheng, M.C. Wang, J. Wang, Quantitative Imaging of Glutathione in Live Cells Using a Reversible Reaction-Based Ratiometric Fluorescent Probe, ACS Chem. Biol. 10 (2015) 864-874.

Journal Pre-proof

[49] Z. Liu, X. Zhou, Y. Miao, Y. Hu, N. Kwon, X. Wu, J. Yoon, A Reversible Fluorescent Probe for Real-Time Quantitative Monitoring of Cellular Glutathione, Angew. Chem.Int. Ed. 56 (2017) 5812-5816.

Journal Pre-proof

Journal Pre-proof

Credit Author Statement

Guoxing Yin: Conceptualization, Writing - original draft, Methodology, Investigation, Formal analysis.

Yabing Gan and Meiling Liu: Investigation, Validation.

Youyu Zhang, Haitao Li and Shouzhuo Yao: Writing - Review & Editing.

Ting Yu, Li Zhou and Peng Yin: Supervision, conceptualization, funding acquisition, project administration.

Journal Pre-proof

Declaration of interests

■ The authors declare that they have no known competing financial interests or personal relationships that could have appeared to influence the work reported in this paper.

■The authors declare the following financial interests/personal relationships which may be considered as potential competing interests:

Declarations of interest: none

Journal Pre-proof

Graphical abstract

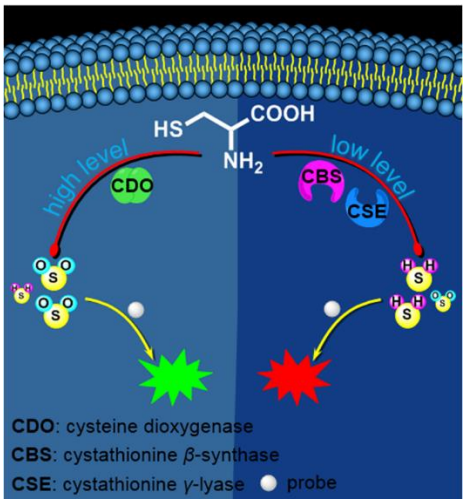

Journal Pre-proof

Highlights

- A novel fluorescent probe for simultaneously monitoring metabolisms of cysteine was developed.
- The probe could simultaneously differentiate SO_2 and H_2S through two different fluorescence channels with similar reaction kinetic and both "off-on" fluorescence responses.
- The probe was successfully applied to monitor and visualize the metabolism pathways of cysteine in living cells and zebrafishes in real time.

Journal Pre-proof